A Switching-Mode Single-Stage Dual-Output Regulating Rectifier Achieving 92.33% Efficiency and Extended Range for Wireless Power Transfer

Lu, Tianqi; Du, Sijun

DOI
10.1109/ESSERC62670.2024.10719538

Publication date
2024

Document Version
Final published version

Published in
ESSERC 2024 - Proceedings

2024 IEEE European Solid-State Electronics Research Conference (ESSERC) | 979-8-3503-8813-8/24/$31.00 ©2024 IEEE | DOI: 10.1109/ESSERC62670.2024.10719538

A Switching-Mode Single-Stage Dual-Output Regulating Rectifier Achieving 92.33% Efficiency and Extended Range for Wireless Power Transfer

Tianqi Lu and Sijun Du
Department of Microelectronics, Delft University of Technology, Delft, The Netherlands
Email: sijun.du@tudelft.nl

***Abstract*—This paper presents a Switching-Mode Regulating Rectifier (SM-RR) with single-stage dual-output regulation for biomedical wireless power transfer applications. To achieve both a high power conversion efficiency (PCE) and a long power transfer distance, the proposed SM-RR can seamlessly switch its operation between voltage mode and resonant current mode. To meet multi-power-rail requirements in loading circuits, it employs only three power transistors to provide two regulated outputs with parallel pulse-frequency modulation, which achieves unobservable cross-regulations. The prototype chip, fabricated in a 180nm CMOS process, achieves two regulated outputs at 1.8V and 3.3V, respectively, up-to-92.33% PCE, and up-to-42% transfer range extension compared to conventional voltage-mode receivers.**

***Index Terms*—Wireless power transfer, regulating rectifier, switching mode, extended range, single stage, dual output.**

I. Introduction

Biomedical implants have gained significant popularity in recent years, especially for applications like neural recording and stimulation. These implants necessitate an onboard power source for functionality, commonly supplied by wirelessly charged batteries or real-time battery-free wireless power transfer (WPT). Nonetheless, due to the restricted space available within the implant, achieving the desired power density and ensuring reliability under varying inductive coupling conditions pose notable challenges.

In a biomedical WPT system, as shown in Fig. 1, the wireless power receiver (RX) typically involves a voltage-mode (VM) rectifier (like a full-bridge) and a DC-DC converter, which performs energy rectification and voltage regulation in separate stages. Despite robust output regulation, it suffers from high system cost/volume and cascaded power losses. To mitigate the drawbacks, VM single-stage regulating rectifiers were proposed, resulting in fewer power components and remarkable power conversion efficiency (PCE) [1]. However, unlike the two-stage structure that can do impedance transformation, the low voltage conversion ratio (VCR) of these single-stage structures sets a high input power threshold, which limits their performance in low coupling-coefficient (k) situations. To address this, resonant current-mode (CM) rectifiers were proposed to enhance VCR with a resonant energy accumulation phase, which significantly lowers the power threshold for low-k cases [2]. However, the resonant phase introduces over-voltage risks and high conduction losses

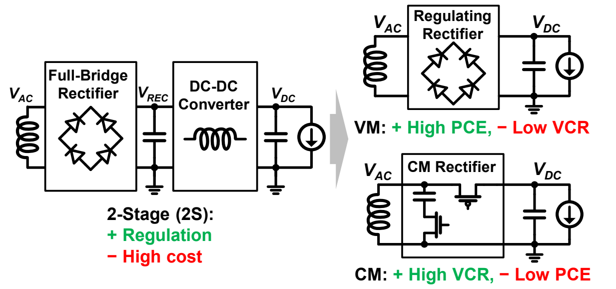

Fig. 1: Conventional 2-stage, VM and CM RX topologies in biomedical WPT systems.

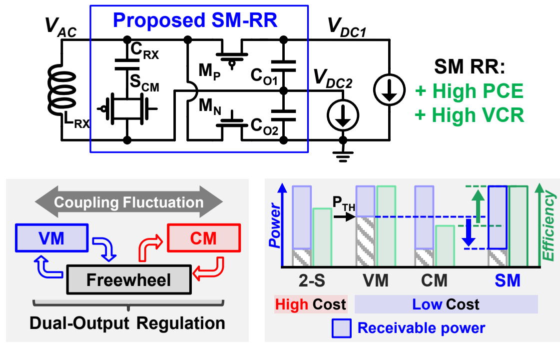

Fig. 2: The proposed switching-mode regulating rectifier (SM-RR) with single-stage dual-output regulation.

in strong coupling cases [3], [4], degrading the output power and PCE consequently. On the other hand, more and more bio-implants require multiple power supplies to power various blocks inside their system, e.g., a low-voltage supply for analog and digital core circuits and a high-voltage supply for stimulation drivers. Unfortunately, most state-of-the-art works only support one output, which necessitates additional parallel power paths or DC-DC converters to generate more regulated outputs [3]. Existing single-stage dual-output designs are mostly derived from VM full-bridge structures [5]–[7], which, however, demand numerous power transistors (PT) and face difficulties dealing with largely varying-k situations.

This paper proposes a single-stage dual-output regulating rectifier, which adaptively switches its operation between VM and CM to accommodate k variations and optimize the trade-

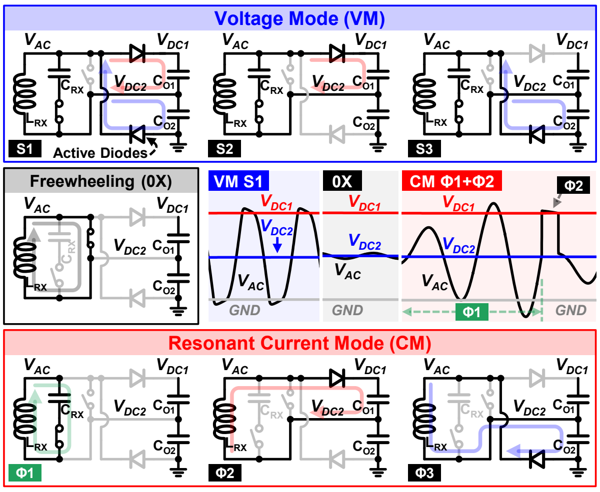

Fig. 3: Operational principles of the proposed SM-RR.

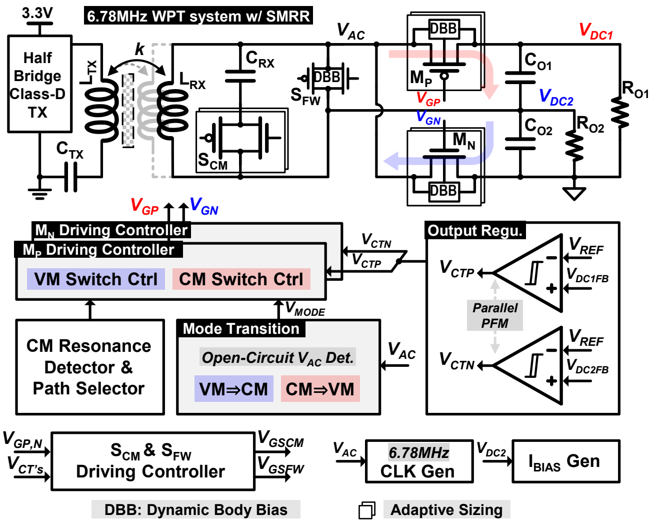

Fig. 4: System architecture of the proposed SM-RR.

off between PCE and VCR. Section II shows the topology and operational principle of the proposed rectifier. The system architecture and circuit implementations are presented in Section III. The measurement results are discussed in Section IV, and Section V gives the conclusion.

II. Proposed Switching-Mode Regulating Rectifier (SM-RR)

Fig. 2 shows the proposed switching-mode regulating rectifier (SM-RR). The VM regulating voltage doubler (RVD) structure brings an inherent VCR of 2, and an additional switch S_{CM} enables the CM operation. Hence, SM-RR is capable of: 1) operating in the VM (as a RVD) in strong coupling cases for high PCE; 2) seamlessly switching to the CM mode in weak coupling cases for extended-range power transfer; 3) periodically entering the freewheeling (0X) mode based on the dual-output regulation to achieve global power control.

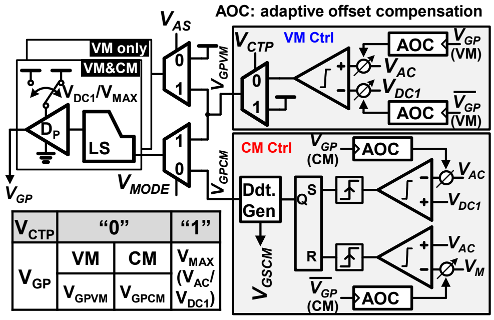

Fig. 5: Implementation of the M_P driving controller.

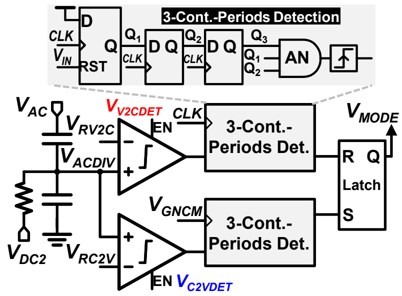

Fig. 6: Implementation of the mode transition detector.

Fig. 3 illustrates the operational principle of SM-RR. The parallel pulse-frequency modulation (PPFM) strategy is utilized to achieve dual-output regulation with unnoticeable cross-regulation [8]. V_{DC1} is regulated by enabling/disabling the high-side PT in the power stage, while V_{DC2} is regulated by enabling/disabling the low-side PT. Thus, the VM operation has three states. In S1, SM-RR charges both C_{O1} and C_{O2}; in S2 (or S3) it charges C_{O1} (or C_{O2}) only. Similarly, the CM operation combines Φ1 (the resonating phase) with Φ2 (the C_{O1}-charging phase) or Φ3 (the C_{O2}-charging phase) to build up the voltage on C_{O1} or C_{O2}, respectively. In the 0X mode, no output capacitor needs to be charged up, and L_{RX} is freewheeling with near-zero loop current, generating a load-shift-keying signal for RX-to-transmitter (TX) communication.

III. System and Circuit Implementations

Fig. 4 shows the system diagram of SM-RR. The power stage consists of three PTs, S_{CM}, M_P, and M_N, with adaptive width sizing for distinct VM and CM operations. M_P, M_N, and S_{FW} have dynamic body bias (DBB) and adaptive gate bias to isolate high voltage swings in their OFF states. The PPFM output regulation is realized by two hysteresis comparators, whose outputs, V_{CTP} and V_{CTN}, go to the switch-driving controllers. The mode transition seamlessly switches the operation of SM-RR between VM and CM, based on the open-circuit V_{AC} detection, which will be detailed later.

Fig. 5 shows the M_P driving controller, which includes both VM and CM controllers. The CM controller also generates a signal V_{GSCM} to drive the PT, S_{CM}, with a deadtime between Φ1 and Φ2/Φ3. To achieve zero-voltage turn-on/-off of PTs, adaptive offset compensation (AOC) is adopted

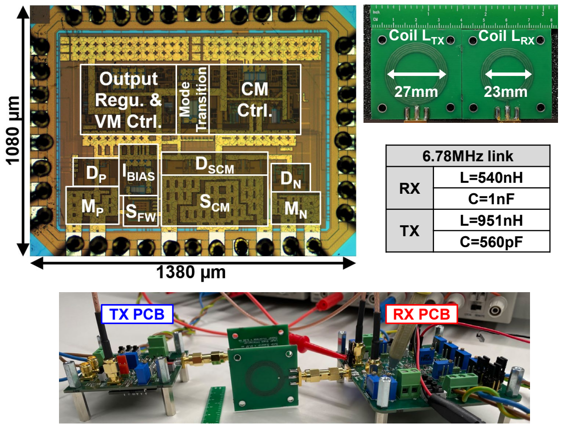

6.78MHz link	
RX	L=540nH
	C=1nF
TX	L=951nH
	C=560pF

Fig. 7: Chip photo of SM-RR and the experimental setup.

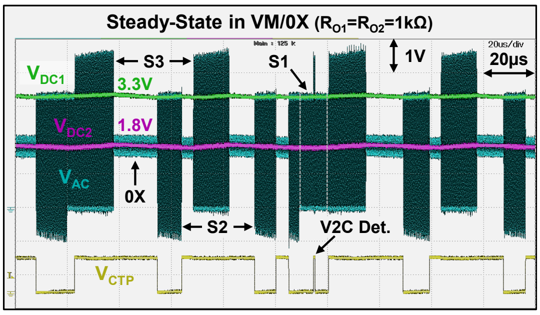

(a) waveforms showing dual-output regulation in VM.

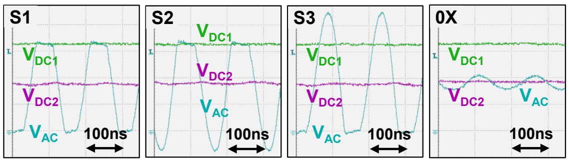

(b) Zoomed-in waveforms of different states.

Fig. 8: Voltage-mode steady-state waveforms of SM-RR.

in both controllers with fast digital-assisted feedback loops. The supply rail of the M_P gate driver, D_P, switches between V_{DC1} and V_{MAX} to achieve adaptive gate bias of M_P.

Fig. 6 shows the mode transition detector, which monitors V_{AC} when V_{V2CDET} or V_{C2VDET} is "1". Once V_{AC} goes lower than V_{RV2C} for 3 consecutive periods in VM, it triggers a VM-to-CM transition. A similar rule applies to the CM-to-VM transition. V_{V2CDET} becomes "1" when SM-RR is in VM S3. For a timely transition, SM-RR can periodically switch to S3 for 5 switching periods (T_{SW}) after it stays in S1 over 40 T_{SW}. When SM-RR is in CM, V_{C2VDET} becomes "1" in each first positive half cycle in CM Φ1 after Φ3. In both VM S3 and CM Φ1, SM-RR can interface a freely resonating L_{RX}-C_{RX} tank in positive half cycles, resulting in open-circuit V_{AC} monitoring for accurate input power detection.

IV. Experimental Results

The proposed SM-RR was designed and fabricated in a 180-nm CMOS process, occupying an active chip area of $0.68\,mm^2$. The chip photo and the measurement setup are shown in Fig. 7. The off-chip components at RX include L_{RX} (540 nH), C_{RX} (1 nF), and $C_{O1,O2}$ (2.2 μF each). The power is emitted from a 6.78 MHz half-bridge class-D TX with pulse-skipping power control. The distance between the TX and RX coils is adjustable to mimic varying coupling conditions.

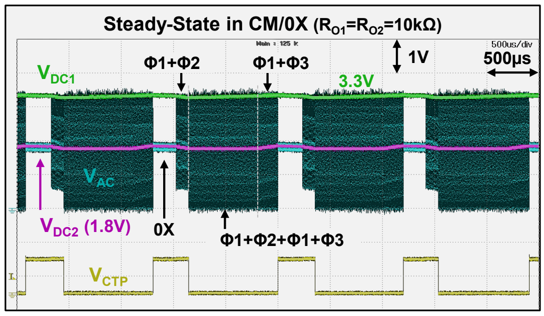

(a) waveforms showing dual-output regulation in CM.

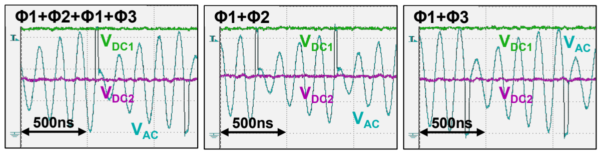

(b) Zoomed-in waveforms of different phases.

Fig. 9: Current-mode steady-state waveformvof SM-RR.

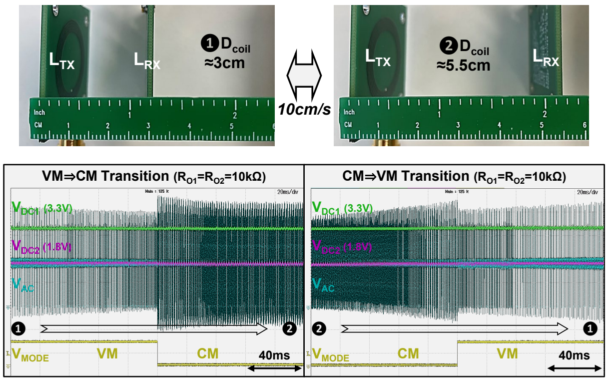

Fig. 10: Mode transition behavior of SM-RR.

Fig. 8(a) shows the steady-state waveforms of the proposed SM-RR when it is operating in VM and regulating the two outputs by four different states (S1-3, 0X). The two outputs, V_{DC1} and V_{DC2}, are regulated at 3.3 V and 1.8 V, respectively. Fig. 8(b) shows the zoomed-in waveforms of the three VM states and 0X case. Fig. 9(a) shows the steady-state waveforms of SM-RR operating in CM, with the zoomed-in three CM phases shown in Fig. 9(b). Thanks to the AOC-based switching control and the PPFM, smooth rectification and tight output regulation can be observed in both modes. Fig. 10 shows the mode transitions when the distance between TX and RX coils changes from 3 cm to 5.5 cm and vice versa. Seamless bidirectional mode transitions can be observed while the two outputs are robustly regulated, benefiting from the open-circuit V_{AC} based mode-transition detection.

TABLE I: Comparison with state-of-the-art designs

	ISSCC'23 [5]	ISSCC'24 [6]	JSSC'23 [7]	TCAS-I'23 [4]	ISSCC'16 [2]	ISSCC'17 [3]	**This work**
Technology	65nm	180nm	180nm	180nm	180nm	350nm	**180nm**
Frequency	40.68MHz	2MHz	6.78MHz	6.78MHz	0.05MHz	1MHz	**6.78MHz**
Operation Mode	VM	VM	VM	CM	CM	VM-CM	**VM-CM**
Number of Outputs (Voltages)	2 (1.1V, 2.2V)	3 (1-3.5V, 4.5V)	2 (3.7V, 5V)	2 (1.8V, 3V)	1	1 (3.2V)	**2 (1.8V, 3.3V)**
Number of PTs	5	8	7	5	2	3	**3**
Regulation Method	PFM	PWM	PFM	Hysteresis	No	Reverse Current	**PPFM**
Cross Regulation	Unobservable	N/R	N/R	N/R	N/A	N/A	**Unobservable**
Adaptive Delay Compensation	Turn-on	N/A	Turn-on/off	Turn-on/off	No	No	**Turn-on/off**
Low-Power Receiving	No	No	No	Yes	Yes	Yes	**Yes**
Max. Transfer Distance (L_{TX}; L_{RX})	N/R	N/R	3mm (1.89μH; 1.87μH)	2cm (1.5μH; 265nH)	8.5cm (6.5μH; 7.2mH)	13.5cm (250μH; 4.4uH)	**7.5cm (951nH; 540nH)**
Max. $P_{OUT,TOT}$	60.5mW	136mW	300mW	7mW	1.7μW	20mW	**171mW**
Peak PCE	90.1%	90.8%	91.8%	85.1%	61.2%	77%	**92.33%**

N/R: not reported; N/A: not applied.

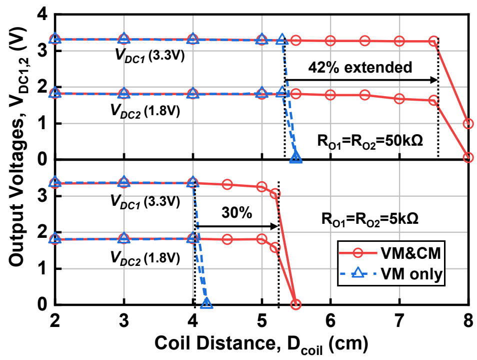

Fig. 11: Measured output voltages at different coil distances.

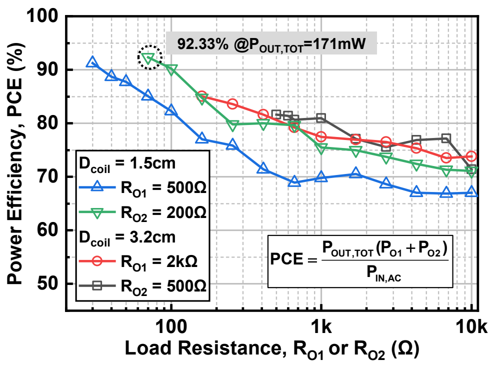

Fig. 12: Measured PCE at different coil distances and loads.

Fig. 11 reveals the voltage retention performance of the two outputs when increasing the coil distance, D_{coil}, i.e. decreasing k. When the two outputs are loaded with 50 kΩ resistors (top plot), the conventional VM-only operation cannot sustain the two outputs with D_{coil} larger than 5.3 cm. In comparison, engaging the proposed switching-mode operation (VM-to-CM) can sustain the two outputs until D_{coil} is 7.5 cm, showing a 42% transfer range extension. When the two outputs are loaded with 5 kΩ resistors (bottom plot), the proposed SM-RR still shows a range extension of 30%.

Fig. 12 shows the measured PCE of the proposed SM-RR with different load resistances and coil distances. The PCE was calculated from the sum of the measured power consumed in both outputs divided by the RX input power. The measurement shows that a peak PCE of 92.33% is achieved when the total output power is 171 mW. Table I compares the proposed SM-RR with state-of-the-art RX designs. This work employs only three power transistors to achieve dual-output regulation, with an extended power transfer distance of up to 7.5 cm. It also shows the highest peak PCE with a good level of output power, meeting the needs of most biomedical implants.

V. Conclusion

This paper presents a single-stage dual-output regulating rectifier capable of both VM and CM operations. Using only 3 PTs, the proposed SM-RR provides 2 regulated outputs at 1.8V and 3.3V, respectively. SM-RR achieves a peak PCE of 92.33% with a peak output power of 171 mW. Thanks to the switching-mode operation, it realizes up-to-42% transfer range extension compared to typical VM-only operation, demonstrating its potential for varying-link WPT use cases.

References

[1] Z. Luo and H. Lee, "A 40.68mhz active rectifier with cycle-based on/off-delay compensation for biomedical implants," in *ESSCIRC*, 2021.

[2] M. Choi, T. Jang, J. Jeong, S. Jeong, D. Blaauw, and D. Sylvester, "A resonant current-mode wireless power receiver and battery charger with 32 dbm sensitivity for implantable systems," *IEEE Journal of Solid-State Circuits*, vol. 51, no. 12, pp. 2880–2892, 2016.

[3] H. S. Gougheri and M. Kiani, "22.3 adaptive reconfigurable voltage/current-mode power management with self-regulation for extended-range inductive power transmission," in *ISSCC*, 2017.

[4] D.-H. Yao, T.-N. Liu, M. Takamiya, and P.-H. Chen, "A 6.78-mhz wireless power transfer system with dual-output resonant current-mode regulating rectifier and transmission power regulation," *IEEE Transactions on Circuits and Systems I: Regular Papers*, vol. 70, no. 12, 2023.

[5] Z. Luo, J. Liu, and H. Lee, "30.9 a 90%-efficiency 40.68mhz single-stage dual-output regulating rectifier with zvs and synchronous pfm control for wireless powering," in *ISSCC*, 2023, pp. 454–456.

[6] H.-S. Lee, K. Eom, and H.-M. Lee, "27.3 a 90.8%-efficiency simo resonant regulating rectifier generating 3 outputs in a half cycle with distributed multi-phase control for wirelessly-powered implantable devices," in *ISSCC*, 2024, pp. 448–450.

[7] F.-B. Yang, D.-H. Yao, and P.-H. Chen, "A quad-mode structure-reconfigurable regulating rectifier with shared-inductor dc–dc energy recycling in a wireless power receiver," *IEEE Journal of Solid-State Circuits*, pp. 1–9, 2023.

[8] T. Lu, K. A. A. Makinwa, and S. Du, "A single-stage dual-output regulating voltage doubler for wireless power transfer," *IEEE Journal of Solid-State Circuits*, pp. 1–12, 2024.